

## Supporting Information

### Surface Polymerization Induced Locomotion

Miguel A. Ramos-Docampo,<sup>a</sup> Edit Brodzkij,<sup>a</sup> Marcel Ceccato,<sup>a</sup> Morten Foss,<sup>a</sup> Mads Folkjær,<sup>b</sup> Nina Lock,<sup>b</sup> and Brigitte Städler<sup>\*a</sup>

<sup>a</sup>Interdisciplinary Nanoscience Center, Aarhus University, Gustav Wieds Vej 14, 8000 Aarhus, Denmark.

<sup>b</sup>Carbon Dioxide Activation Center (CADIAC), Department of Biological and Chemical Engineering, Aarhus University, Åbogade 40, 8200 Aarhus N, Denmark.

<sup>\*</sup>bstadler@inano.au.dk

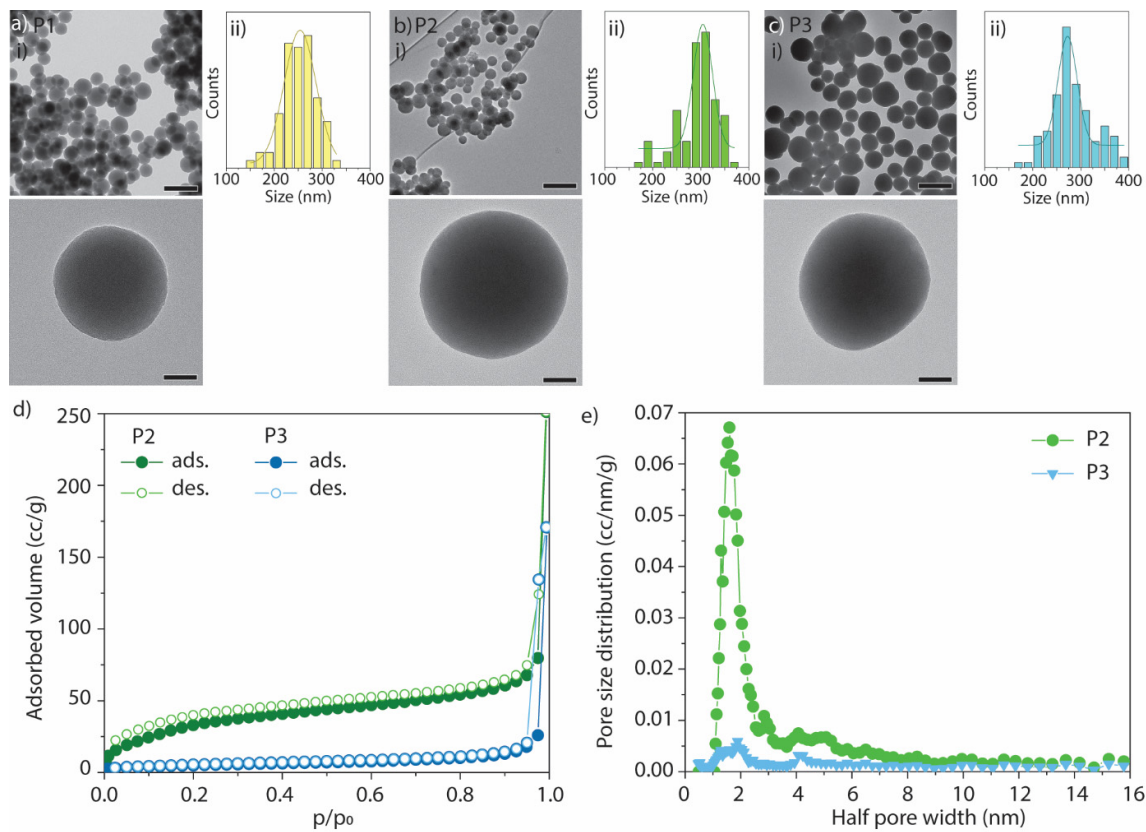


**Figure S1. Synthesis of the silica nanoparticles.** Silica nanoparticles with different size and density (porosity) were prepared and visualized by TEM (ai, bi and ci). Scale bars are 500 nm (upper panel) and 50 nm (lower panel). The size distribution was fit to a Gaussian curve (aii, bii and cii). The porosity of the particles was assessed by  $N_2$  adsorption–desorption (close and open symbols, respectively) isotherms, showing in both cases a type II isotherm typical of non-porous materials. However, P2 adsorbed more gas due to its much higher surface area (d). The pore size distribution indicated that sample P2 has relevant mesopores while P3 may be considered non-porous (e).

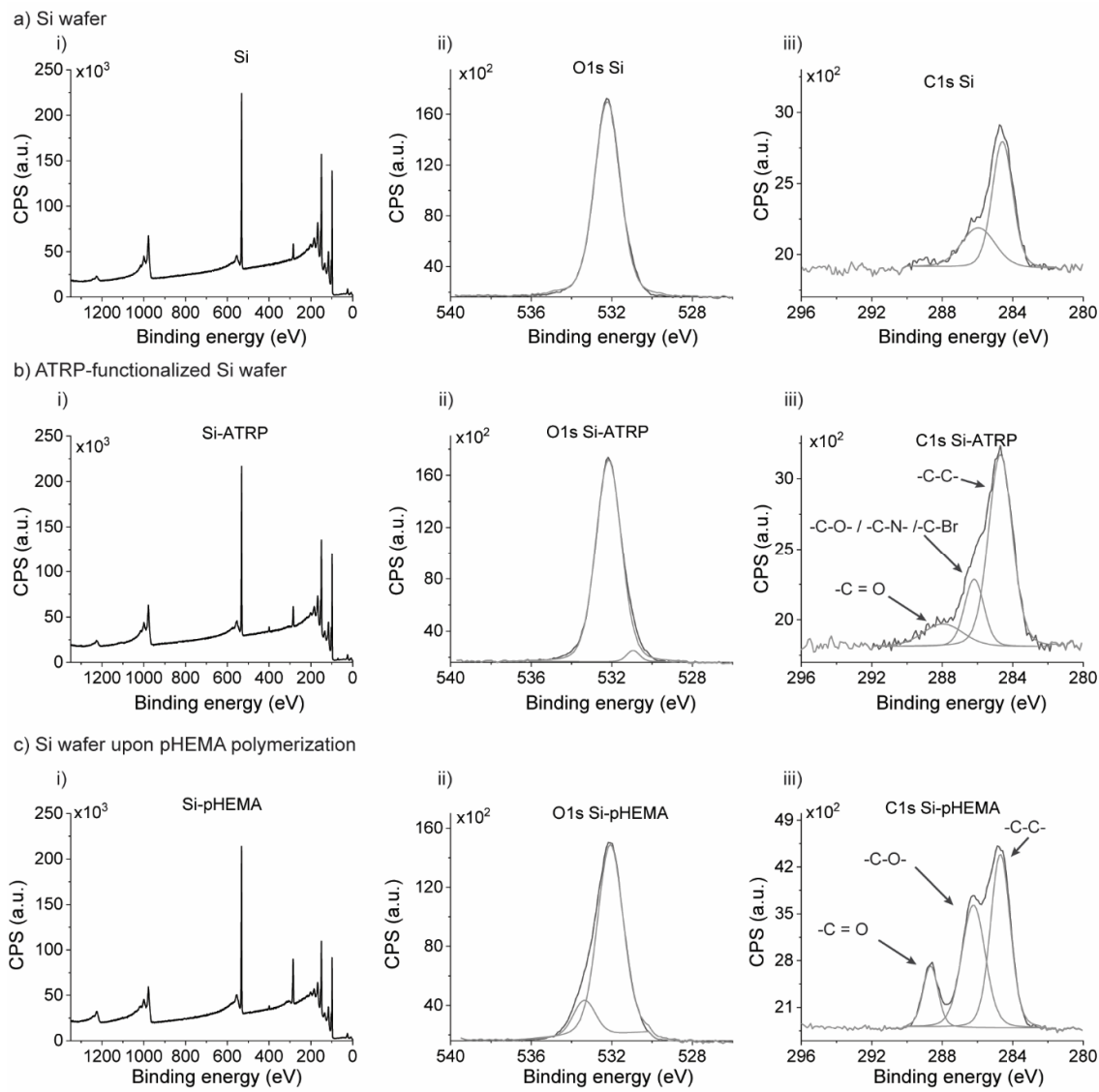


**Figure S2. XPS analysis of polymerization at planar surfaces.** The characterization was carried out for the silicon wafers (a), the ATRP-functionalized surfaces (b) and upon polymerization of pHEMA after 60 min (c). Survey spectra were collected to have an overview of the sample (ai, bi and ci). Next, high resolution spectra of oxygen 1s (aii, bii and cii) and carbon 1s (aiii, biii and ciii) allowed for a detailed investigation of the ATRP initiator deposition as well as for the polymerization process.

**Table S1.** Atomic percentage of elements analysed by XPS in planar surfaces.

Element	Atomic percentage (%)						
	Si wafer	ATRP-functionalized Si wafer	Si wafer upon pHEMA polymerization				
			0.5 h	1 h	2 h	4 h	24 h
O	29.3	33.1	31.9	32.1	30.2	31.0	30.0
C	8.33	13.9	22.0	33.2	44.3	41.2	43.6
N	0.34	1.45	1.35	0.80	2.09	2.24	9.50
Si	62.3	51.4	44.7	34.2	23.2	26.4	16.9
Br	-	0.16	-	-	-	-	-

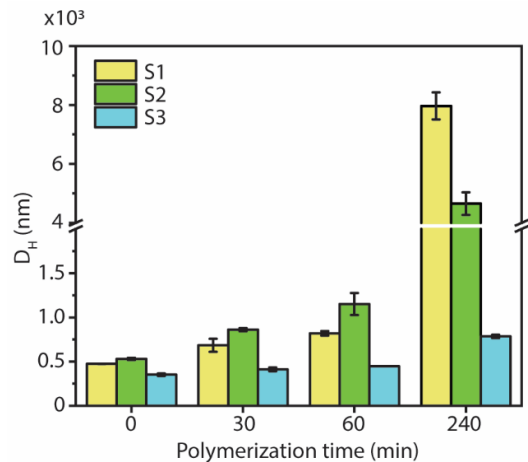


**Figure S3.** Hydrodynamic diameter ( $D_H$ ) of M1, M2 and M3 after 30, 60 and 240 min of polymerization. Note that time 0 refers to S1, S2 and S3 (no polymerization). There was a linear relation between  $D_H$  and polymerization over 60 min of polymerization. After 240 min of polymerization, M1 and M2 seemed to aggregate, therefore, we focused the mobility assessment to shorter times.

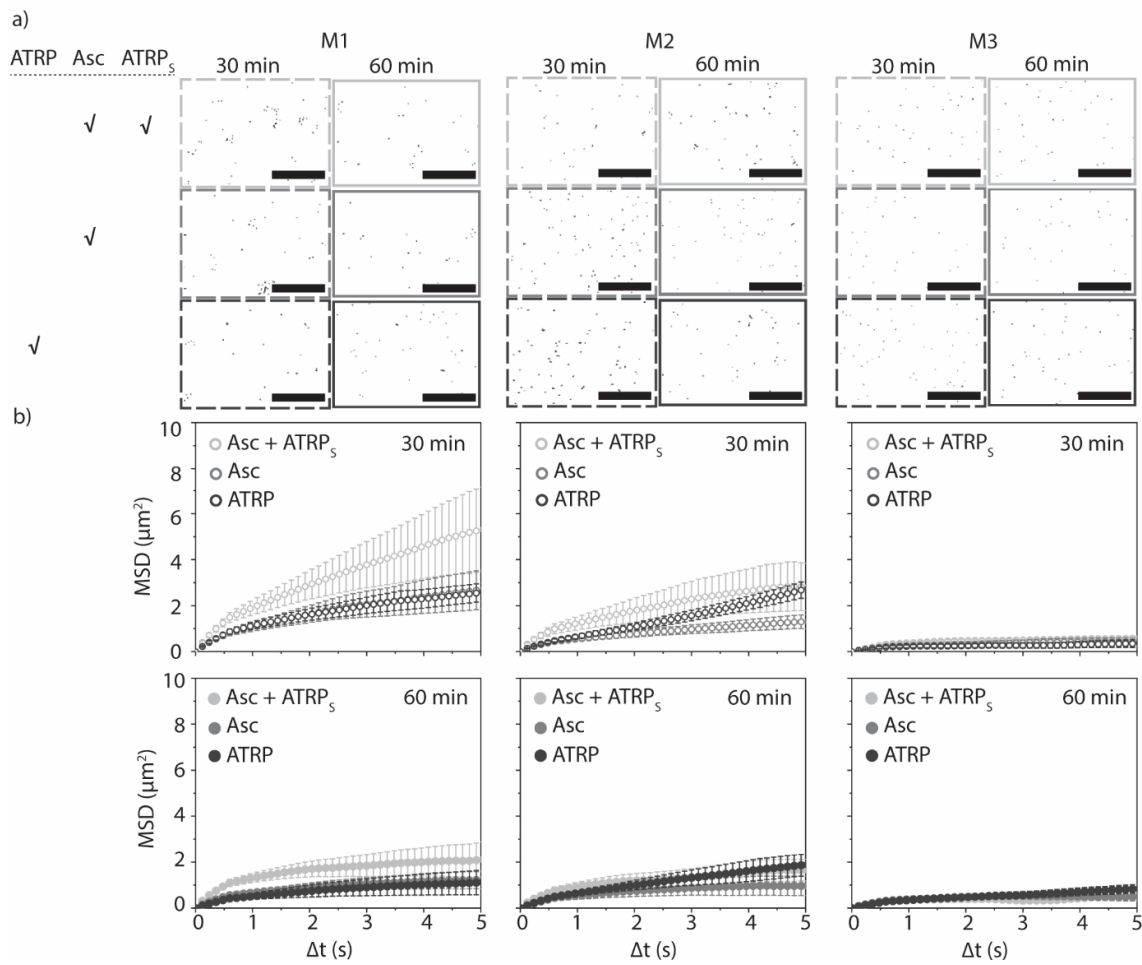


**Figure S4. Control experiments of M1, M2 and M3.** (a) Extracted trajectories and (b) MSD plots of the control motors after 30 min (open symbols) and 60 min (close symbols) of polymerization in different environmental conditions. Scale bars are 100  $\mu\text{m}$ .

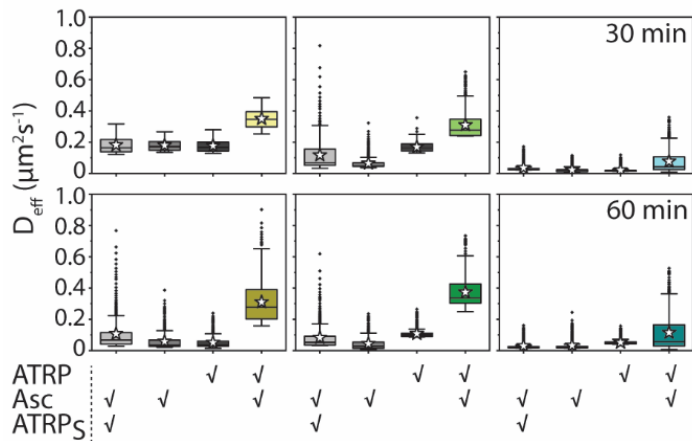


**Figure S5. Whisker plots of M1, M2 and M3.** The diffusion coefficients of the motors were evaluated after 30 and 60 min of polymerization in different conditions. The whisker plots demonstrated that the average velocity (star) and the median velocity (line crossing each box) did not overlap, which was a sign of asymmetric velocity distributions with tendency towards the population being dominated by slower motors (since median < mean). However, the extended size of the boxes in the whisker plots, where the lower and upper edges of a box mark the first and third quartile of the velocity distribution, respectively, suggested that the populations of fast motors were significant. Moreover, a fraction of very fast motors with velocities well above the average velocity of an ensemble was revealed (whiskers and cross symbols). It was further observed that the asymmetry of the distributions increased with increasing polymerization time, when the mean and median become less similar and not centred in the box.

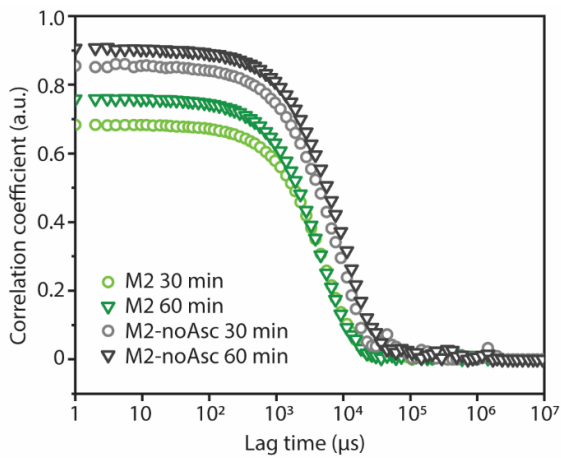


**Figure S6. Correlograms of M2.** Correlograms of M2 in the presence of the polymerization mixture were obtained using DLS after 30 min and 60 min. M2-noAsc were used as controls. The shift towards shorter lag times indicated motors moved faster than controls.

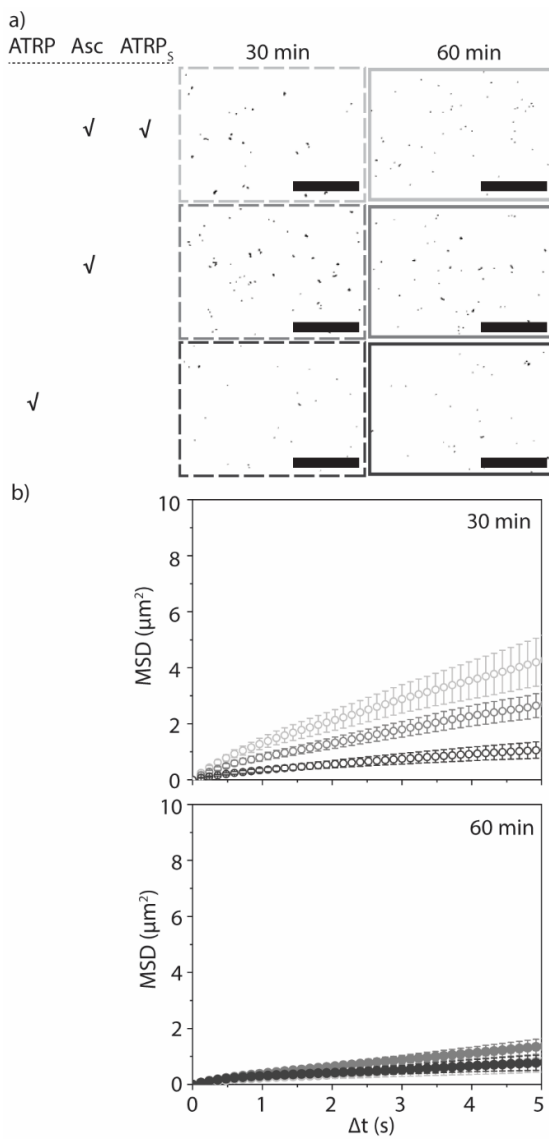


**Figure S7. Control experiments of JM2.** (a) Extracted trajectories and (b) MSD plots of control JM2 after 30 min (open symbols) and 60 min (close symbols) of polymerization in different environmental conditions. Scale bars are 100  $\mu\text{m}$ .

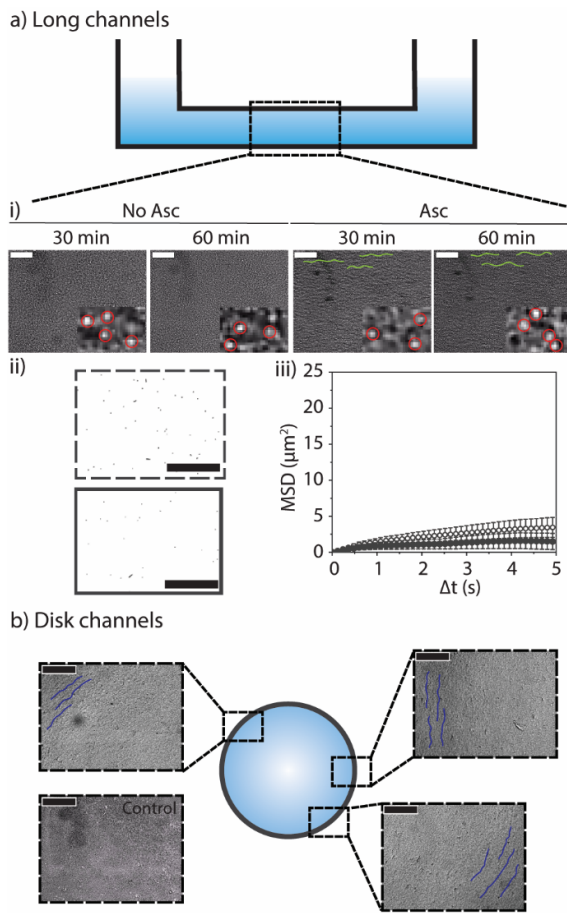


**Figure S8. Control experiment of M2 at high motor concentration.** (a) Locomotion in long-shaped channels. (i) Bright-field microscopy images of the motor in the absence and presence of ascorbate upon 30 and 60 min polymerization. In the presence of ascorbate, the homogeneous motors move in the shape of waves (in green). Insets show a magnification of the same picture. Red circles denote motors. Scale bars are 100  $\mu\text{m}$ . (ii) Trajectory maps and (iii) MSD plots of the control experiments in the absence of ascorbate upon 30 min (open symbols) and 60 min (close symbols). Scale bars are 100  $\mu\text{m}$ . (b) Locomotion in disk-like channels. The motors tend to move in the direction parallel to the channel wall (trajectories shown in blue).

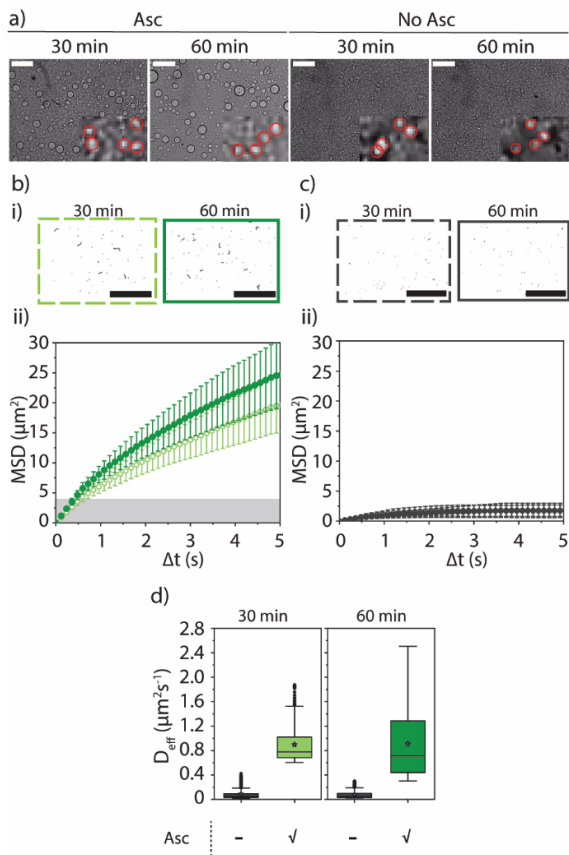


**Figure S9. M2 locomotion at high motor and HEMA concentrations.** (a) Bright-field microscopy images of the motor in the absence and presence of ascorbate upon 30 and 60 min polymerization. Red circles denote motors. Scale bars are 100  $\mu\text{m}$ . Locomotion in the (b) presence and (c) absence of ascorbate. Trajectory maps (bi and ci) and MSD plots (bii and cii) of M2 after 30 (dashed frames and open symbols) and 60 (solid frames and solid symbols) min of polymerization. The grey area in the MSD plots indicates the range of the controls for each experiment. Scale bars are 10  $\mu\text{m}$ . (d) Whisker plots of the effective diffusion coefficients ( $D_{\text{eff}}$ ) of M2 in the absence and presence of ascorbate after 30 (left) and 60 (right) min of polymerization.

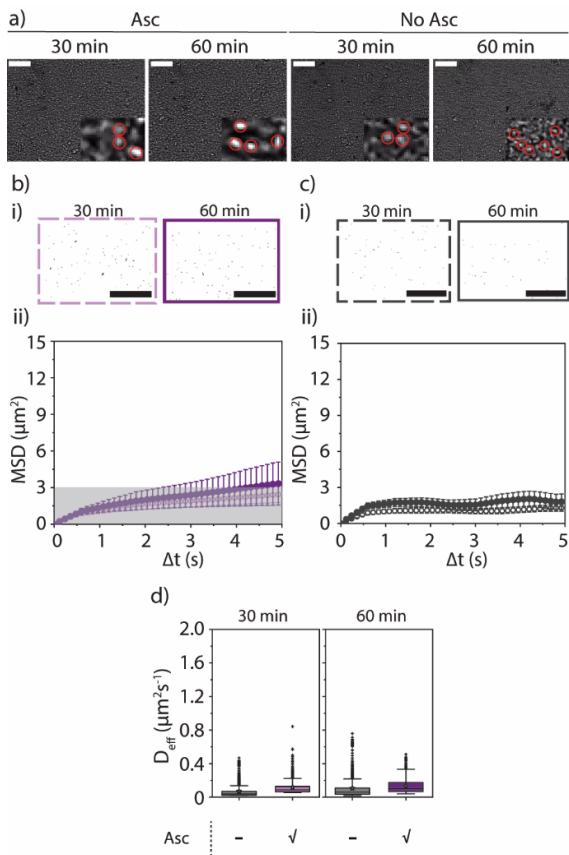


**Figure S10. JM2 locomotion at high motor concentration.** (a) Bright-field microscopy images of the motor in the absence and presence of ascorbate upon 30 and 60 min polymerization. Red circles denote motors. Scale bars are 100  $\mu\text{m}$ . Locomotion in the (b) presence and (c) absence of ascorbate. Trajectory maps (bi and ci) and MSD plots (bii and cii) of JM2 after 30 (dashed frames and open symbols) and 60 (solid frames and solid symbols) min of polymerization. The grey area in the MSD plots indicates the range of the controls for each experiment. Scale bars are 10  $\mu\text{m}$ . (d) Whisker plots of the effective diffusion coefficients ( $D_{\text{eff}}$ ) of JM2 in the absence and presence of ascorbate after 30 (left) and 60 (right) min of polymerization.